Supplementary Materials

In vivo biocompatibility, biodistribution and therapeutic efficiency of titania coated upconversion nanoparticles for photodynamic therapy of solid oral cancers

Sasidharan Swarnalatha Lucky[1,2], *Niagara Muhammad Idris*[2], *Kai Huang*[2], *Jaejung Kim*[2], *Zhengquan Li*[3], *Patricia Soo Ping Thong*[4], *Rong Xu*[5], *Khee Chee Soo*[4], *Yong Zhang*[2,6*]

[1]NUS Graduate School for Integrative Sciences & Engineering (NGS), Singapore 117456

[2]Department of Biomedical Engineering, National University of Singapore, Singapore 117575

[3]Institute of Physical Chemistry, Zhejiang Normal University, P. R. China 321004

[4]Division of Medical Sciences, National Cancer Centre Singapore, Singapore 169610

[5]School of Chemical & Biomedical Engineering, Nanyang Technological University, Singapore 637459

[6]College of Chemistry and Life Sciences, Zhejiang Normal University, P. R. China 321004

[*]Corresponding author: biezy@nus.edu.sg

EXPERIMENTAL METHODS

Detection of EGFR expression in OSCC cells and tumor.

Immunofluorescence: Cells were seeded in 8-well chambered slide at a cell density of 25 x 10^3 cells per well and incubated overnight. The cells were then fixed in ice-cold methanol, followed by blocking with a blocking buffer (2 % goat serum, 2% BSA, 0.1% Tween 20) for 1 h at 37°C. Subsequently, the cells were incubated with primary anti-EGFR antibody (clone EP38Y) diluted 1:100 in blocking buffer (Abcam, Cambridge, UK), at RT for 2h. The sections were washed 3 X 5 min with PBS and then incubated with Texas red (TR) labelled secondary antibody (goat polyclonal antibody (Abcam, UK), diluted 1:1000 in blocking buffer for 1h at RT in dark. Following a 3 X 5 min washing with PBS, the plasma membrane of the cells were stained with Wheat Germ Agglutinin, Alexa Fluor® 488 Conjugate (Molecular Probes, Inc., USA) at a concentration of 5 μg/ml for 10 min at RT. The nucleus was further counterstained with Hoechst 33342 stain (Molecular Probes, Inc., USA) at a concentration of 1 μM for 5 min. The cells were gently washed thrice with PBS and mounted using Vectashield mounting medium (Vector Laboratories, CA, USA). EGFR expressing human epidermoid cancer cells A431 was used as the internal positive control, while human breast adenocarcinoma MCF-7 cells served as the negative control. The cells were imaged using an upright Nikon 80i Fluorescence Microscope (Nikon, Tokyo, Japan) equipped with a 980 nm Laser Wide-field Fluorescence add-on (EINST Technology Pte Ltd, Singapore) using a 20X objective (200X magnification). The EGFR statining, plasma membrane and nuclei were visualized under excitation with Hg arc lamp and a standard DAPI, FITC and TRITC filter set respectively.

Western blotting: The cells were grown in 175 mm^3 flask and once confluent they were lysed by adding cell lysis buffer (M-PER, Pierce, USA) along with protease inhibitor (Complete

Mini, Roche, Germany). The lysate was centrifuged at 14,000 *g* for 15 min at 4°C and the supernatnant was carefully aliquoted and stored at -80°C. To prepare tumor lysates, OSCC xenograft tumors were excised and immediately frozen in liquid nitrogen. The tumors were then crushed into powder in liquid nitrogen and ice-cold lysis buffer (TPER, Pierce, IL, USA) with protease inhibitor and kept on ice for 30 min. After subsequent centrifugation, the supernatant (total tumor cell lysates) were stored at -70°C. The protein concentration was estimated by Bradford's assay using Bio-Rad protein assay reagent in accordance with the manufacturer's protocol. 100 μg of protein were resolved on 10% SDS-PAGE gel before transferring to a nitrocellulose membrane. The membrane was then probed with 1:200 anti-EGFR monoclonal antibody (Cell Signaling Technology, USA) or anti-β actin polyclonal antibody (Abcam, USA) and 1:400 horseradish peroxidase-conjugated antibody (Cell Signaling Technology, USA) using the iBind Western System (Life Technologies, USA). The membrane was then incubated with chemiluminescent substrate (Thermo Fisher Scientific, USA) followed by detection on traditional ECL film (Amersham Hyperfilm ECL, GE Healthcare, USA). The intensity of the band was quantified using NIH Image J 1.49p software (National Institute of Health, USA). The ratio of EGFR band intensity was plotted against actin bands.

Comparison of *in vitro* targeting and uptake of Anti-EGFR-PEG-TiO_2-UCNs.

To compare the targeting efficiency of anti-EGFR-PEG-TiO_2-UCN, nanoparticles were incubated with various EGFR overexpressing cell-lines such as OSCC, A431, H596 and H460 and low EGFR expressing MCF-7 and HepG2 cells. Cells were seeded in 8 well chambered slide and incubated overnight; following which the cells were treated with anti-EGFR-PEG-TiO_2-UCNs at a concentration of 1 mM for 3 h. Thereafter the cells were washed, fixed and stained as mentioned above. The UCN uptake was quantified by taking the blue (UCN fluorescence) to red (nuclei) intensities of the images. Furthermore, the uptake

dynamics of anti-EGFR-PEG-TiO_2-UCNs in OSCC and MCF-7 cells was determined by incubating the nanoparticles with the cells at various time-points.

Long term toxicity study – Animal weight measurements.

Twenty five animals were used in this study. Animals were randomly grouped in to 5 groups of 5 animals and each group was housed separately. All animals were weighed before treatment (Day 1). Animals in the control group received no treatment. Group 2 to 5 received intravenous injection of different doses of anti-EGFR-PEG-TiO_2-UCN ranging from 10 -200 mg/kg (volume of injection= 100 ul). Following systemic administration of the nanoparticles, the animals were closely monitored for the first 48 h, and then daily once for 28 days, during when they were observed for any physiological or behavioral changes as well as mortality. The animals were weighed individually every day and the food and water intake of each group were also recorded daily up to 28 days.

Immunohistochemistry.

Tumor tissue samples were fixed in 10% formalin for 24 h, and then processed using a tissue processor (Leica TP 1020, Germany) and embedded in paraffin. The paraffin embedded samples were cut using a microtome (Leica RM 2135, Germany) at 5 μm thickness. The sections were mounted on superfrost/plus slides (Fischer Scientific, USA) and air-dried. On the day of staining the slides, the paraffin was cleared in Neo-clear (Merck Millipore, USA) twice for 10 min before rehydrating in ethanol series. Following 10 min incubation with hydrogen peroxide to block the endogenous peroxidase activity, the sections were incubated overnight at 4°C with primary antibodies, Ki-67 (1:100; Abcam, USA).. To confirm the specificity of binding, normal mouse serum IgG1 (1:500) was used as a negative control. Following extensive washing, sections were incubated for 30 min in the secondary biotinylated antibody, rinsed and followed by DAB Chromogen (Vector Laboratories, UK)

for 10 min. Sections were then counter-stained with Harris's hematoxylin and dehydrated in ascending grades of ethanol before clearing in xylene and mounting with a cover slip. Images were captured using a Nikon 80i Fluorescence Microscope (Nikon, Tokyo, Japan) using a 20X objective (200X magnification). Image J (1.49p, National institute of Health, USA) software was used to analyze and quantify the percentage of Ki-67 staining. For H&E staining, serial 8 μm thick cryosections were fixed in acetone, stained with H&E stain as mentioned elsewhere, and imaged by a Nikon 80i digital microscope (Nikon, Tokyo, Japan) using a 20X objective (200X magnification).

RESULTS

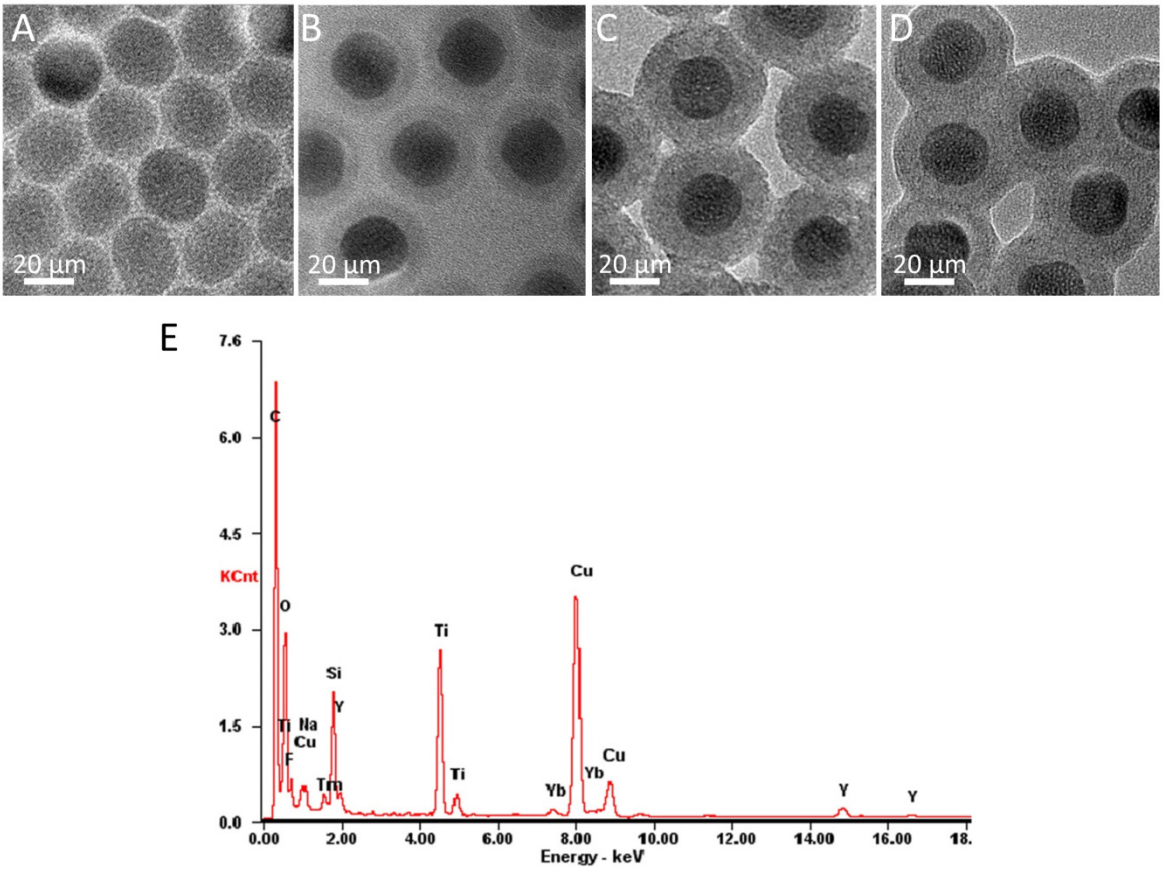

Figure S1. TEM images of nanoparticles at various stages of synthesis: (A) UCN core ($NaYF_4$:Yb,Tm), (B) silica coated UCN ($NaYF_4$:Yb,Tm@SiO_2), (C) TiO_2-UCN (TiO_2 coated $NaYF_4$:Yb,Tm@SiO_2) and (D) anti-EGFR-PEG-TiO_2-UCNs; scale bar: 20 nm. (E) EDX spectrum of TiO_2-UCNs supported on a carbon-film coated copper grid.

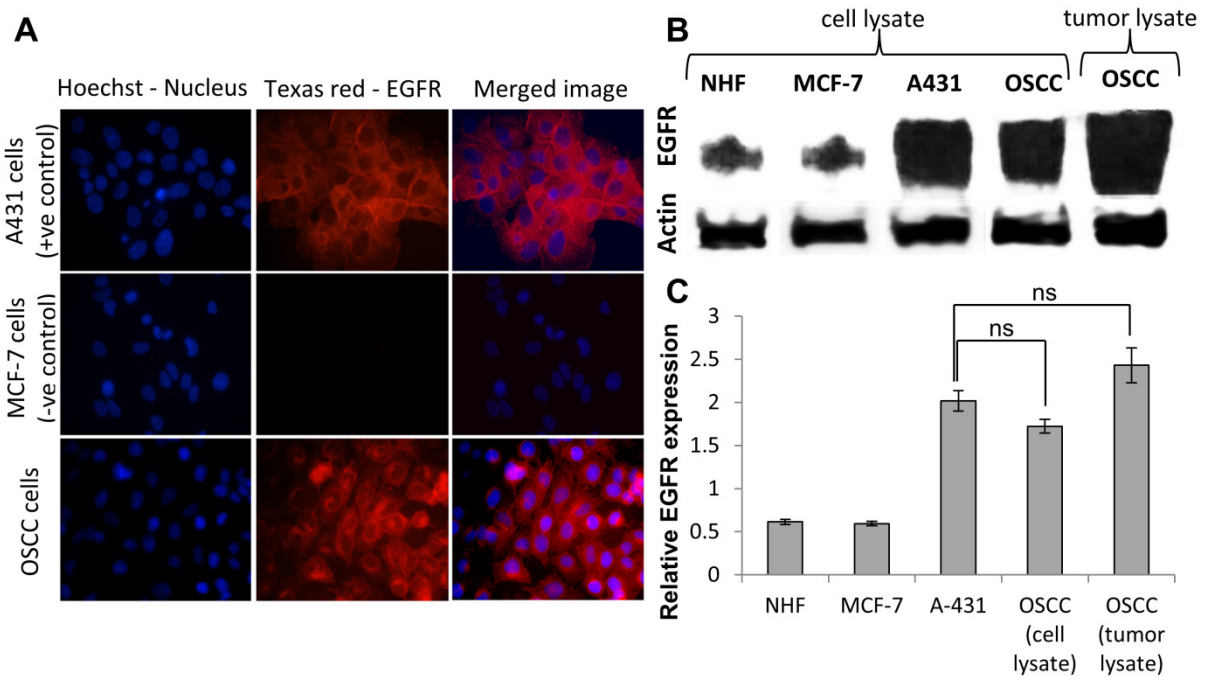

Figure S2. (A) Representative immunofluorescence images showing the expression of EGFR in A431 (positive control), MCF-7 (negative control) and OSCC. Red fluorescence represents EGFR staining and blue fluorescence depicts nuclei stained by Hoechst 33342. (B) Western blot image showing EGFR and actin expression in various cell and tumor lysate. (C) The ratio of EGFR band intensity plotted against actin. Error bars represents standard deviation of the mean; ns stands for 'not significant'.

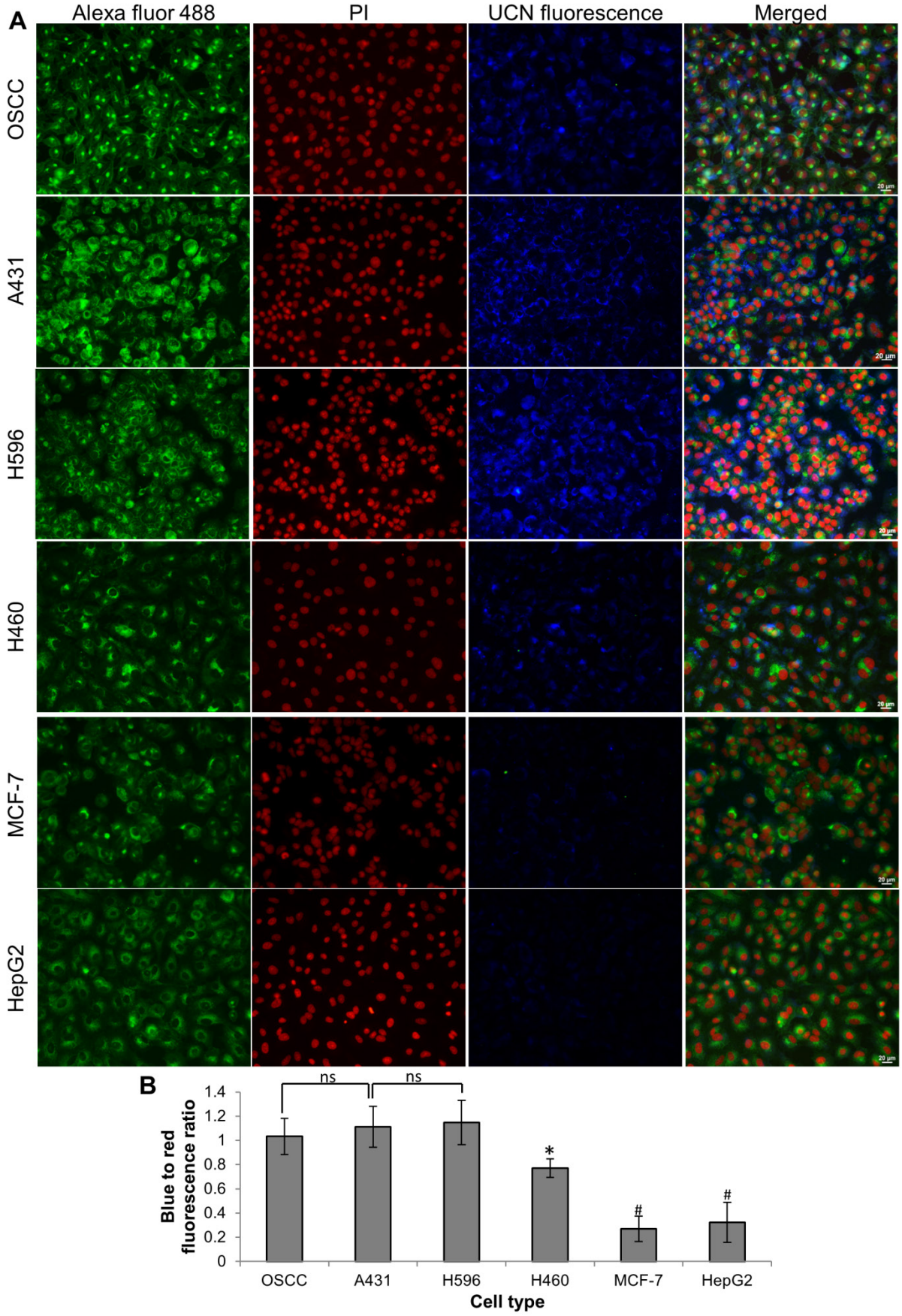

Figure S3. (A) Representative images of anti-EGFR-PEG-TiO_2-UCN uptake (blue fluorescence) in various cells expressing different levels of EGFR receptors post 3 h

incubation; green and red fluorescence indicate cell membrane and nucleus respectively (Magnification 200X, Scale bar: 20 μm). (B) Comparison of fluorescence intensities of 1 mM anti-EGFR-PEG-TiO_2-UCNs internalized by various cells; **P*<0.05, #*P*<0.0001 compared with the uptake of anti-EGFR-PEG-TiO_2-UCN by A431 cells, 'ns' denotes that there is no significant difference between the groups compared; data are mean fluorescence intensities (n>4) ± SD.

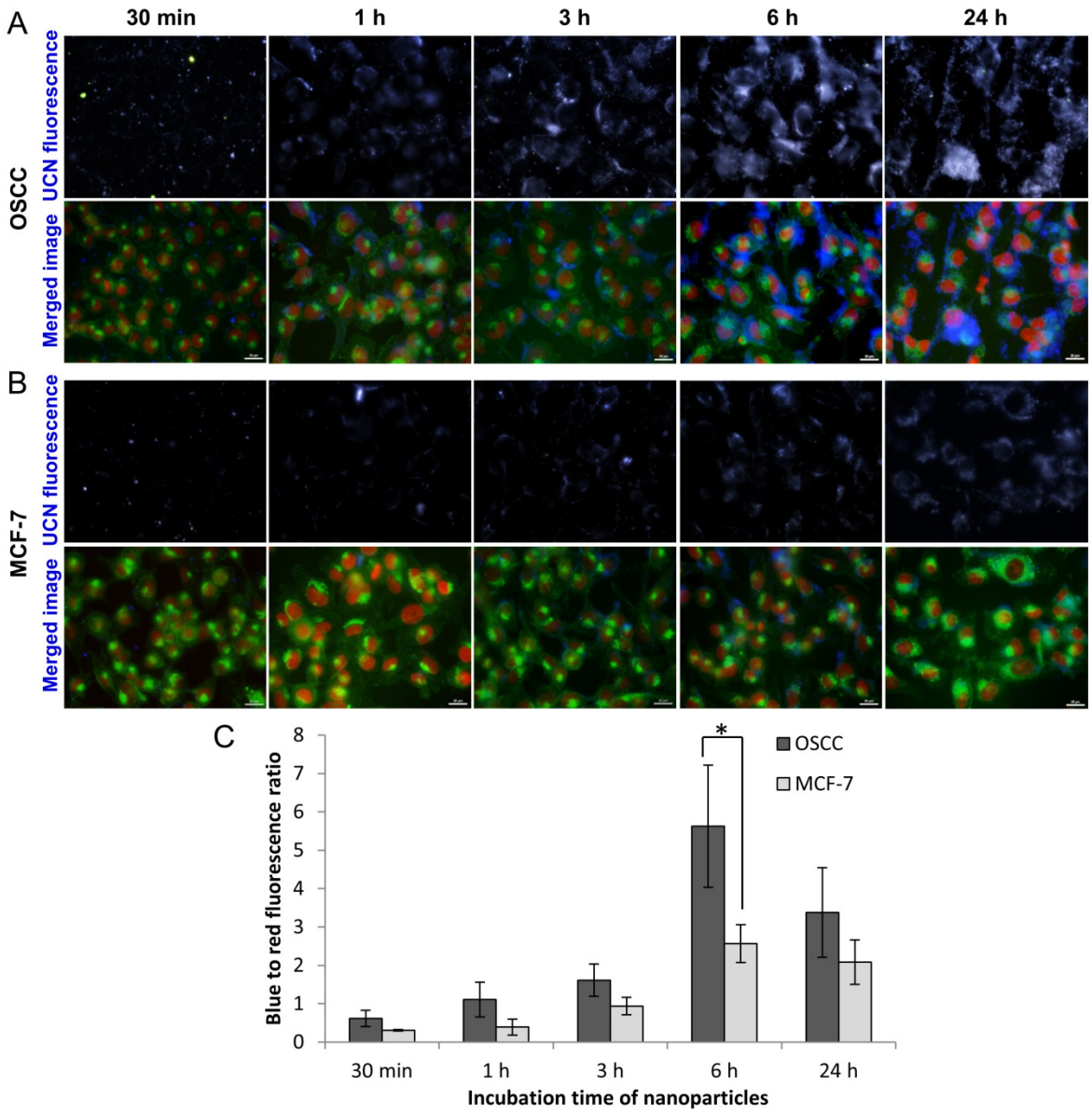

Figure S4. (A) Representative images of anti-EGFR-PEG-TiO_2-UCN uptake at a concentration of 1mM, as a function of time in OSCC and MCF-7 cells; green and red fluorescence indicate cell membrane and nucleus respectively (Magnification 400X, Scale bar: 20 μm). (B) Comparison of fluorescence intensities of anti-EGFR-PEG-TiO_2-UCN internalized by OSCC and MCF-7 cells as a function of time; *P<0.0001 data are mean fluorescence intensities (n>4) ± SD.

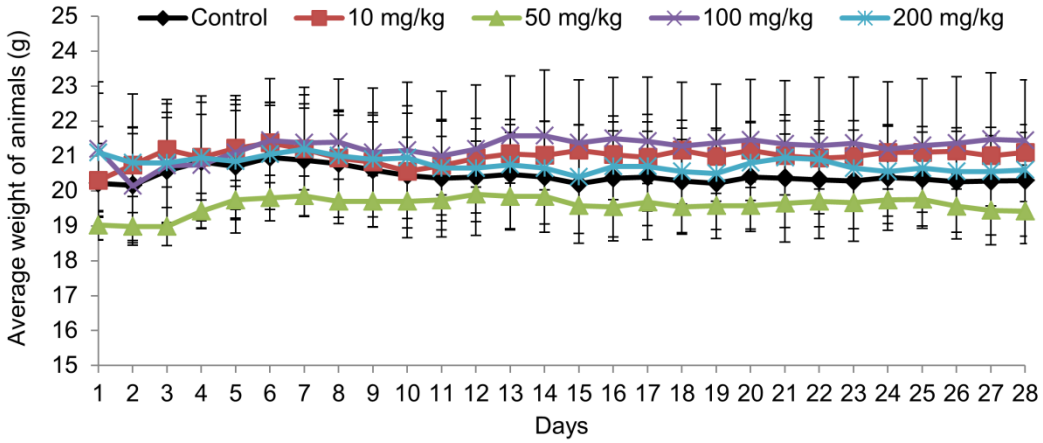

Figure S5. Change in body weight of mice in different groups following intravenous injection of different doses anti-EGFR-PEG-TiO_2-UCNs for up to 28 days. Data are presented as mean ± SD (n = 3-5 per group).

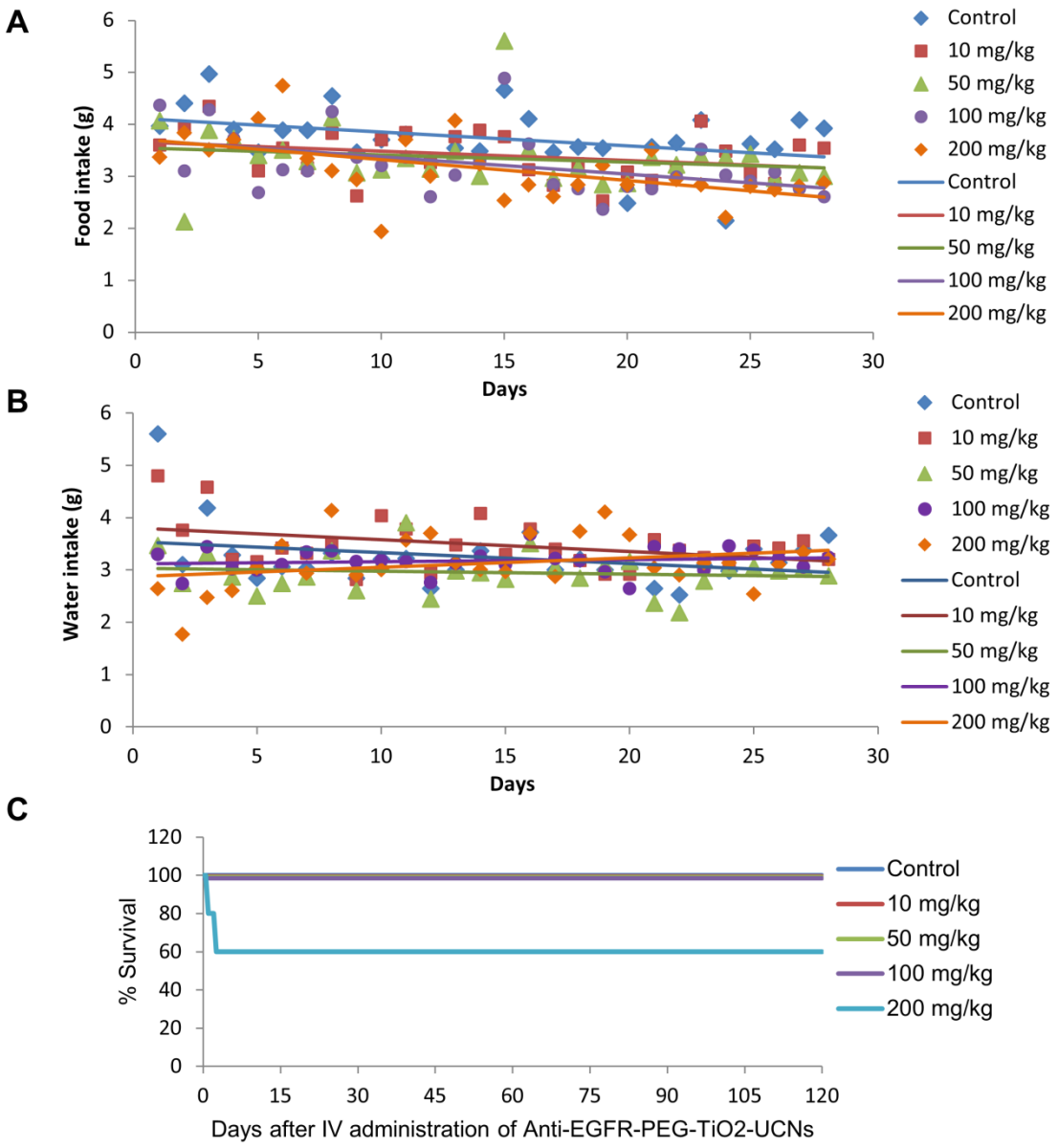

Figure S6. Comparison of food (A) and water (B) intake in animals injected with different dose of anti-EGFR-PEG-TiO_2-UCNs up to a period of 28 days. Data are presented as mean ± SD (n = 3-5 per group). (C) Survival rates of mice in different treatment groups within 120 days. Data are presented as mean ± SD (n = 5 per group).

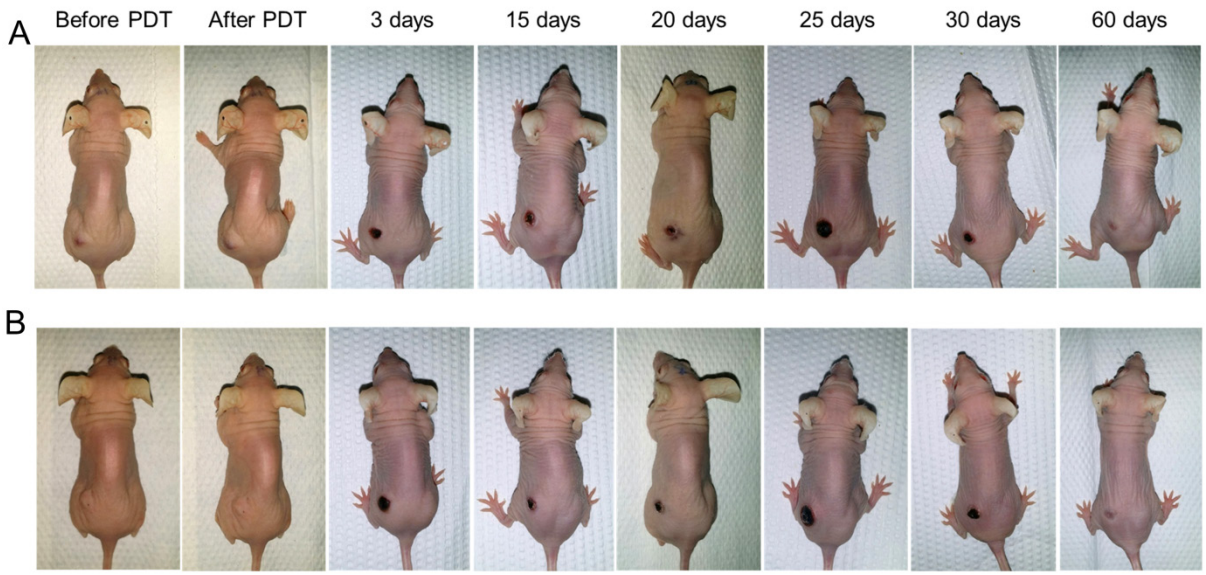

Figure S7. Images of 2 different animals (A) and (B), completely free from tumor burden at 60 days following 3 intratumoral administration of anti-EGFR-PEG-TiO_2-UCN and NIR irradiation sessions (repeat PDT).

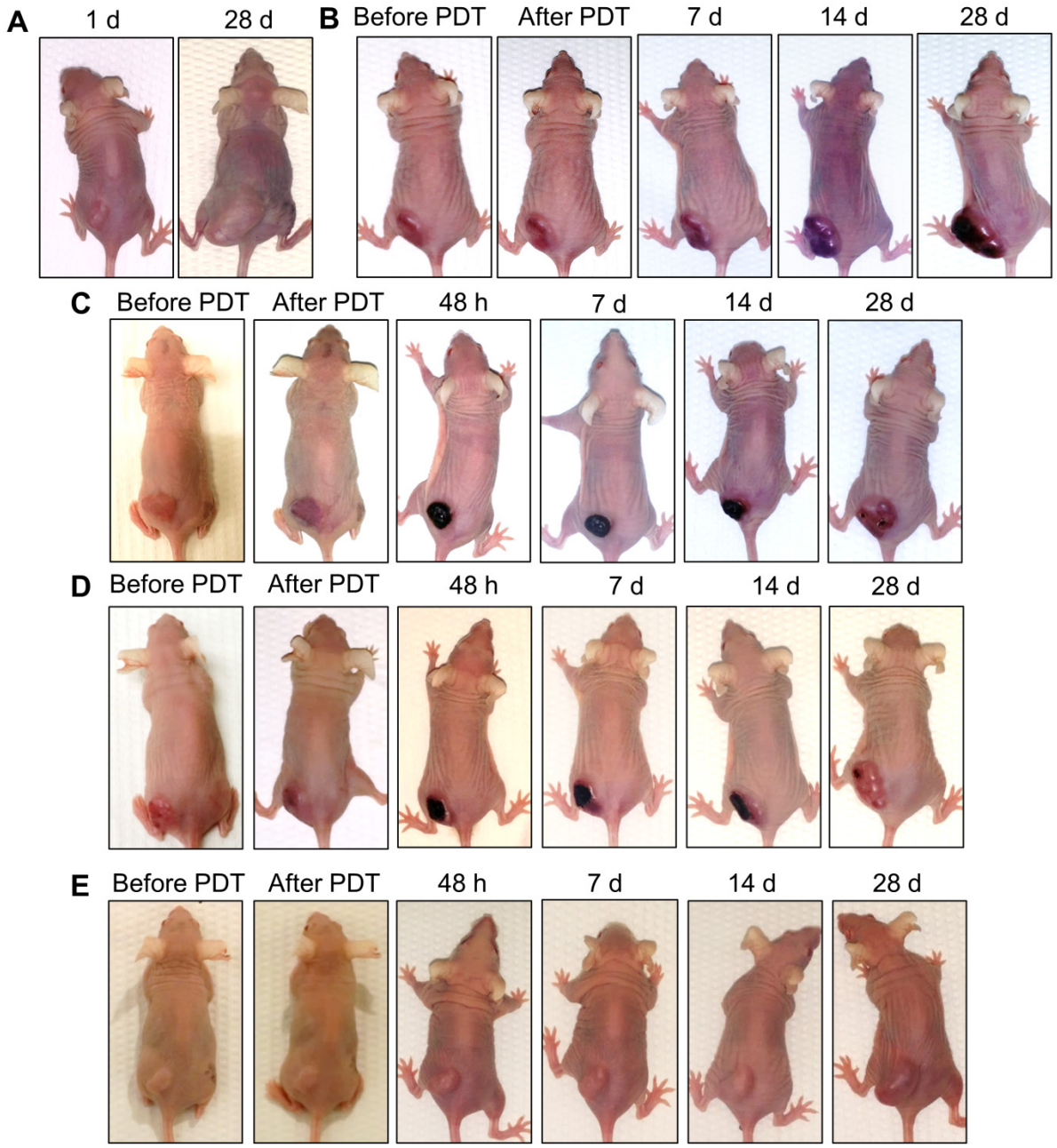

Figure S8. Representative images of mice in different groups: (A) Untreated control, (B) 980 nm NIR light alone (C) anti-EGFR-PEG-TiO_2-UCN + 980 nm light, (D) anti-EGFR-PEG-TiO_2-UCN + 980 nm light + 6 mm tissue phantom, (E) anti-EGFR-PEG-TiO_2-UCN + 980 nm light + 10 mm tissue phantom.

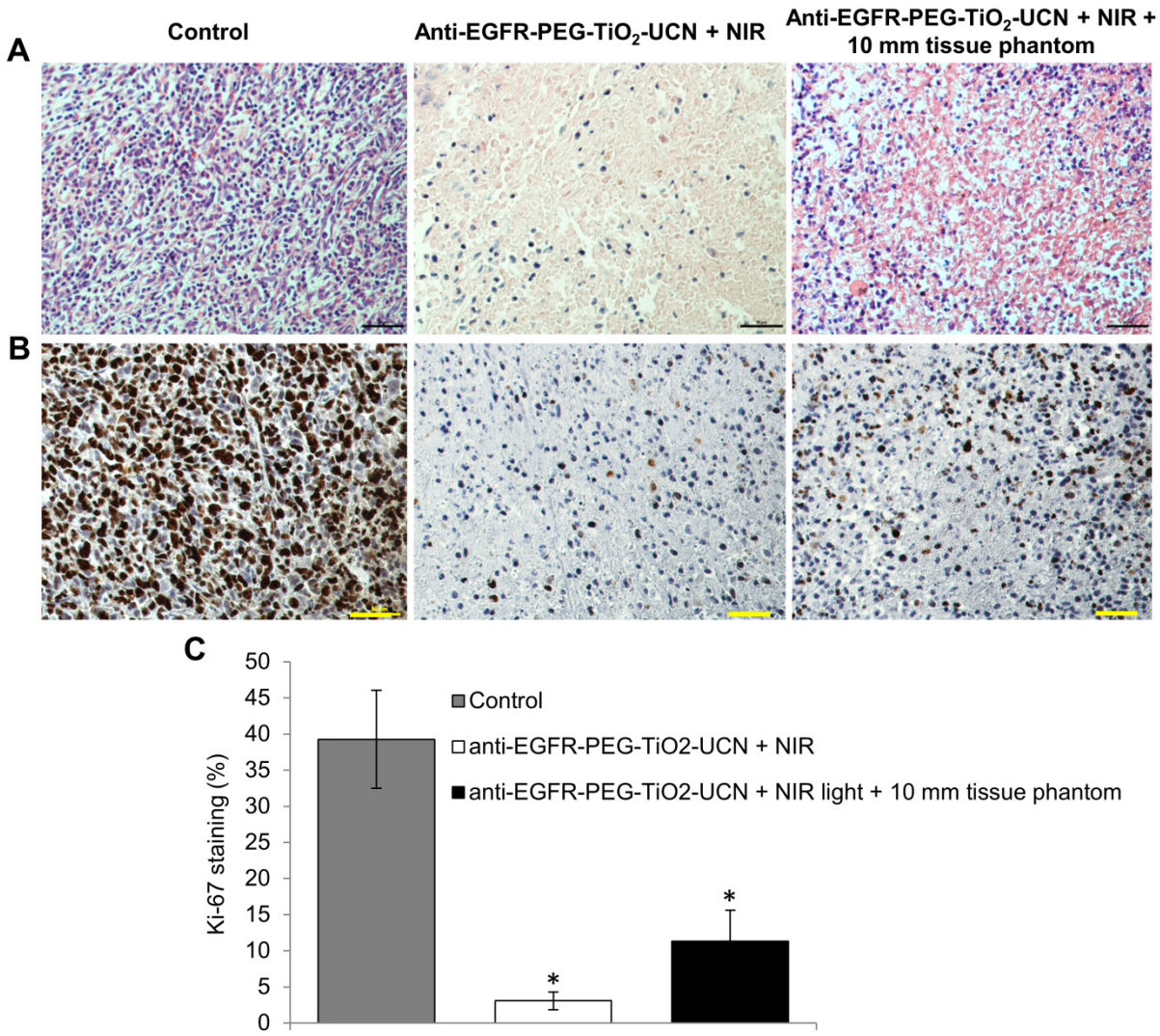

Figure S9. (A) Representative H & E stained images of tumor sections from different groups 15 days after respective treatment. (Scale bar: 50 µm, Magnification: 200X) (B) Representative photomicrograph showing Ki-67 proliferative index in tumor sections from different groups 15 days after respective treatment (Scale bar: 50 µm, Magnification: 200X) (C) Quantitative data for the proliferation index is shown as percent of Ki-67-postive cells, **P*<0.05 compared to control, error bars indicate SD of the mean.